Integration of Scheduling, Design, and Control of Multiproduct Chemical Processes Under Uncertainty

Bhushan P. Patil, Eduardo Maia, and Luis A. Ricardez-Sandoval
Dept. of Chemical Engineering, University of Waterloo, Waterloo, ON, Canada N2L 3G1

DOI 10.1002/aic.14833
Published online April 22, 2015 in Wiley Online Library (wileyonlinelibrary.com)

The development of a methodology that addresses the simultaneous design, scheduling, and control of multiproduct processes is focused. The proposed methodology takes into account the influence of disturbances by the identification of their critical frequency, which is used to quantify the worst-case variability in the controlled variables via frequency response analysis. The uncertainty in the demands of products has also been addressed by creating critical demand scenarios with different probabilities of occurrence, while the nominal stability of the system has been ensured. Two case studies have been developed as applications of the methodology. The first case study focuses on the comparison of classical semisequential approach against the simultaneous methodology developed, while the second case study demonstrates the capability of the methodology in application to a large-scale nonlinear system. © 2015 American Institute of Chemical Engineers *AIChE J*, 61: 2456–2470, 2015
Keywords: design, process control, optimization

Introduction

Multiproduct processes represent an important section of chemical process industry, which focus on production of several types/grades of products. Studies addressing the optimal design of multipurpose/multiproduct processes have been presented in the literature.[1–4] Another key aspect in multiproduct plants is process controllability, which is concerned with the optimal control.[5–8] Moreover, optimal process scheduling is a key subject of relevance for various sectors in the chemical process industry including multiproduct plants. In these processes, various grades of the product are produced and scheduling of the production of the different products affect the process economics and therefore it must be addressed in optimal fashion. Scheduling for multipurpose/multiproduct plants has been reported in the literature, which includes optimal scheduling of various multiproduct processes.[9–17] The purpose of this study is to address all the aspects described above simultaneously for multiproduct plants, that is, design, control, and scheduling. There are two main approaches through which the optimization of chemical processes can be addressed taking into account the three aspects described above. The first approach is to address each aspect one by one, that is, sequentially. In the sequential approach, optimal parameters are calculated for different aspects independent from each other, that is, in sequence, and therefore, there is no integration of the aspects. The solutions obtained through this approach are suboptimal because of the lack of simultaneous consideration of all aspects involved. In the second approach, all the aspects are addressed simultaneously by the integration of all three aspects to achieve the optimal scheduling, design, and control; therefore, this approach is expected to provide more economically attractive results as compared to the first approach.

The integration of design and control has been addressed in many publications including the optimal design and control of various large-scale processes including bioethanol,[18] extractive ditillation,[19] Tennessee Eastman process,[20] sugar cane sulfitation tower,[21] ternary distillation,[22] multigrade polymerization,[23] and styrene polymerization.[24,25] Similarly, several methodologies with different features and limitations for integration of design and control have been proposed in the literature.[26–31] Some of the studies discuss the simultaneous design and control using advanced model-based control techniques such as model predictive control.[32–37] Integration of design and control approaches that has taken model parameter uncertainty into account has also been reported.[38–43] Review papers that summarize the different ways and the development in the area of integrated design and control are also available.[44–48] Besides the integration of design and control, several studies are also available for the integration of design and scheduling for chemical systems. These works include the publications on plants,[49,50] simultaneous design and scheduling in multipurpose plants,[51–54] and in multiproduct plants.[55] The effect of uncertainty has been addressed during the integration of design and scheduling.[56,57] Moreover, studies addressing the simultaneous scheduling and control have been reported. This includes the integration of scheduling and control for batch plants,[58,59] polymerization processes,[60,61] and continuous stirred tank reactor systems (CSTRs).[62,63] There are also studies available that address the integration of scheduling and control in mixed-continuous batch processes,[64] tubular reactors,[65] and

Correspondence concerning this article should be addressed to L. A. Ricardez-Sandoval at laricard@uwaterloo.ca.

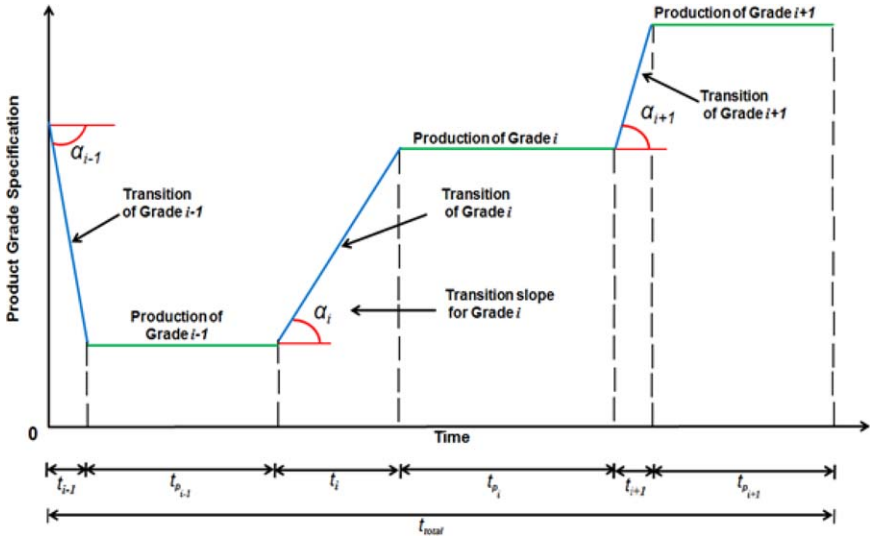

Figure 1. Various product grades in a multiproduct process.

[Color figure can be viewed in the online issue, which is available at wileyonlinelibrary.com.]

multiproduct continuous parallel lines.[66] Engell and Harjunkoski[67] have summarized the possible ways of integration of scheduling and control whereas Harjunkoski et al.[68] have discussed the practical use of the integration of these two aspects.

Apart from the integration of few of the three aspects for chemical processes, to the authors' knowledge, there is only one study on integration of all three aspects that addresses the design, scheduling, and optimal control of a methylmethacrylate polymerization reactor.[69] In that study, the decisions were made on design including steady-state operating conditions and equipment sizing, on scheduling including production sequence and on optimal control. The smooth transitions between grades were part of control decision and were achieved by incorporating process dynamics during transitions. One of the limitations of that study is that the control decisions did not involve the evaluation of controller tuning parameters as no closed-loop control scheme was implemented, that is, the control actions were directly obtained from optimization. In addition, the effect of process disturbances was not considered in that study.

The goal of this study is to present a methodology that takes into account scheduling and control decisions for the optimal process design of multiproduct processes. The key novelty of the work presented here is in the simultaneous consideration of the design, scheduling, and control aspects of the chemical process under the influence of process disturbances and uncertainty in the parameters. The decisions involved in this analysis encompass design parameters, for example, optimal and equipment sizes, control parameters, for example, optimal controller tuning parameters, and scheduling decisions, which include the identification of optimal transition trajectories and the optimal sequence of production for multiproduct processes. Another contribution of the work is the use of ramp functions for the transitions between various grades, where slopes of the ramp functions are a part of the decision variables. The implementation of ramp functions allows the transitions to be smooth, while the slopes of the ramp functions are optimization variables that can potentially minimize the cost associated with the transition between different product grades. An MINLP optimization formulation has been developed which focuses on minimization of overall plant cost in the presence of process constraints while ensuring nominal stability of the system under critical realizations in the disturbances and model parameter uncertainty. To the authors' knowledge, the integration of all these aspects under the conditions mentioned above has not been explicitly addressed in the available literature. Two case studies have been developed to test the proposed methodology. The first case study concentrates on the application of the methodology to a multiproduct CSTR. A comparison has been made to demonstrate the benefits of the proposed simultaneous approach over a semisequential approach, where design and control parameters are evaluated first simultaneously and then the scheduling parameters are generated. The second case study focuses on a large highly nonlinear multiproduct process, that is, high impact polystyrene (HIPS), where multiple grades of the product are produced based on the conversion required under critical realizations in the disturbances and uncertainty in the product demands.

The organization of this article is as follows: the next section presents the problem statement followed by the presentation of the mathematical formulation proposed for the integration of design, scheduling, and control of multiproduct processes. The results and discussion section presents the results on the two case studies used in this work to demonstrate the implementation of the proposed methodology, that is, a CSTR system and a HIPS process. Concluding remarks are presented at the end of this article.

Problem Statement

Consider a multiproduct plant which produces various grades of the product. Each grade has a particular specification and a demand to meet. As shown in Figure 1, the operation consists of production and transition periods for each grade i. During the transition period of a grade i, the required specification of the grade is reached and then the production stage of the grade starts. The production stage is continued until the required demand is met at the required grade specification. Once the required production of the grade i is achieved, transition to grade $i+1$ begins and eventually the production is achieved for that grade. The

procedure is repeated until all the required product grades (I) are produced to meet the product demands. The present study assumes that, once the production wheel is completed, it is immediately and indefinitely repeated. Also, each grade is produced only once in the complete production cycle. As shown in Figure 1, t_i and t_{p_i} represent the transition and production times of grade i, while t_{total} is the time required to complete productions and transitions for all product grades.

All the transitions are assumed to occur following a ramp function to achieve the set point related to specification of the grades. The slope of the ramp (α_i) denotes the transition rate for the i^{th} grade and is part of the optimization variables considered in the presented analysis. Once the transition of grade is completed and the required composition is achieved, the production period starts; the product is assumed to be stored in a product (storage) tank.

The product tank starts filling only after the required specification is achieved, that is, only within the production period, and stops when both the required composition (grade) and demand are achieved. The complete operation is assumed to occur under the influence of critical realizations in the process disturbances, which are assumed to follow an oscillatory behavior, and uncertainty in the system's parameters, for example, production demands.

In the problem under consideration the given are: (a) the actual dynamic nonlinear process model describing the behaviour of a multiproduct process, (b) the process model parameters (e.g., molar flow rate of the feed), (c) the control scheme, (d) the required specifications and demands of the grades to be produced, (e) the disturbance specification, assumed to be sinusoid signal with given amplitude and critical frequency, (f) uncertainty specification in terms of critical scenarios and their probabilities for uncertain parameter, and (g) process constraints to be satisfied during operation. The problem to be formulated aims to determine: (a) the optimal equipment design and steady-state operating conditions for each grade, (b) the optimal tuning parameters for the control scheme, (c) optimal transition slopes for each grade, and (d) optimal sequence of production.

Methodology for Integration of Scheduling, Design, and Control

This section presents the details of the methodology developed for integration of design, scheduling, and control. The description of the features considered in the methodology is presented next along with the mathematical description of the optimization formulation. The notations used to define the present methodology are listed in the notation section of this article.

Parameter uncertainty

The methodology presented in this work explicitly accounts for uncertainty in the process parameters, for example, uncertainty in the demand of products. To account for this condition, the critical uncertain scenarios in the parameters are assumed to be discretized and need to be specified *a priori*, that is

$$\mathbf{w}=[\mathbf{w}^1,\mathbf{w}^2,\ldots,\mathbf{w}^z,\ldots\mathbf{w}^{\text{ns}}] \tag{1}$$

where "ns" denotes the number of critical scenarios to be considered in the analysis; each uncertain scenario $\mathbf{w}^z$ has been assigned with a probability of occurrence P^z.

Process disturbances

In the presented study, each k^{th} process disturbance is specified as follows

$$\boldsymbol{\eta}_k(t)=\boldsymbol{\eta}_{k_{\text{nom}}}+\boldsymbol{\eta}_{k_m}\sin(\omega_{c_{k,i}}t) \tag{2}$$

where $\boldsymbol{\eta}_{k_{\text{nom}}}$ is the nominal operating value of the process disturbance and $\boldsymbol{\eta}_{k_m}$ is the amplitude of the k^{th} process disturbance, which is chosen depending upon the process dynamics, whereas $\omega_{c_{k,i}}$ represents the critical frequency evaluated for each grade i that generates maximum variability in the controlled variables due to critical realizations in the k^{th} disturbance. The critical parameter $\omega_{c_{k,i}}$ is not known *a priori* and will be calculated internally by the present methodology. This is a new feature introduced by the present approach. The response in the l^{th} controlled variable as a result of a sinusoidal process disturbance input is as follows

$$\mathbf{y}_l(t)=\mathbf{y}_{l_{\text{nom}}}+\mathbf{y}_{l_m}\sin(\omega_{c_{k,i}}t+\Phi) \tag{3}$$

where $\mathbf{y}_{l_{\text{nom}}}$ is the nominal operating value of the process disturbance, $\mathbf{y}_{l_m}$ is the amplitude of the controlled variable and Φ is the phase angle by which the l^{th} controlled output is delayed. The largest (worst-case) variability in the controlled variable due to k^{th} disturbance is determined by the frequency of the sine function, that is, $\omega_{c_{k,i}}$. In this work, this critical frequency $\omega_{c_{k,i}}$ is identified from the linearization of the actual nonlinear closed-loop process model ($\mathbf{f}_{\text{closed}}$) around the steady-state operating conditions specified for the production of grade i. The identification of the critical frequency from the actual closed-loop nonlinear process model ($\mathbf{f}_{\text{closed}}$) requires the solution of an intensive optimization formulation, which needs to appear as a constraint in the overall integration of scheduling, design, and control formulation. Therefore, this formulation can become prohibitive for large-scale applications. Thus, the approximation in terms of linearized process model along with frequency response analysis has been used in this work for the identification of the critical frequency ($\omega_{c_{k,i}}$).

Based on the above, the critical frequency $\omega_{c_{k,i}}$ is obtained from the linearized closed-loop process model via frequency response analysis as follows.

The closed-loop process model ($\mathbf{f}_{\text{closed}}$) is linearized around a steady-state operating condition for each product grade i specified as part of decision variables ($\mathbf{d}$) as follows

$$\begin{aligned}\dot{\mathbf{x}}_{\text{lin}}&=\mathbf{A}_i\mathbf{x}+\mathbf{B}_i\boldsymbol{\varphi}\\ \boldsymbol{\Omega}_{\text{lin}}&=\mathbf{C}_i\mathbf{x}+\mathbf{D}_i\boldsymbol{\varphi},\ \forall i=1\ldots I\end{aligned} \tag{4}$$

where $\mathbf{x}_{\text{lin}}$ is the vector of states of the linearized closed-loop process model, $\boldsymbol{\varphi}$ is an input vector which includes the disturbances affecting the process, while $\boldsymbol{\Omega}_{\text{lin}}$ represents the output vector that includes controlled variables calculated from the linearized closed-loop process model. The matrices $\mathbf{A}_i$, $\mathbf{B}_i$, $\mathbf{C}_i$, $\mathbf{D}_i$ are the state matrices of the linearized closed-loop process model. The closed-loop state-space model is identified at each single function evaluation of the optimization formulation for each grade i using the values specified for the optimization variables at each optimization step. The nonlinear closed loop process model can be linearized analytically, for example, using Taylor's series expansion, or from systems identification methods using the traditional least-squares technique.

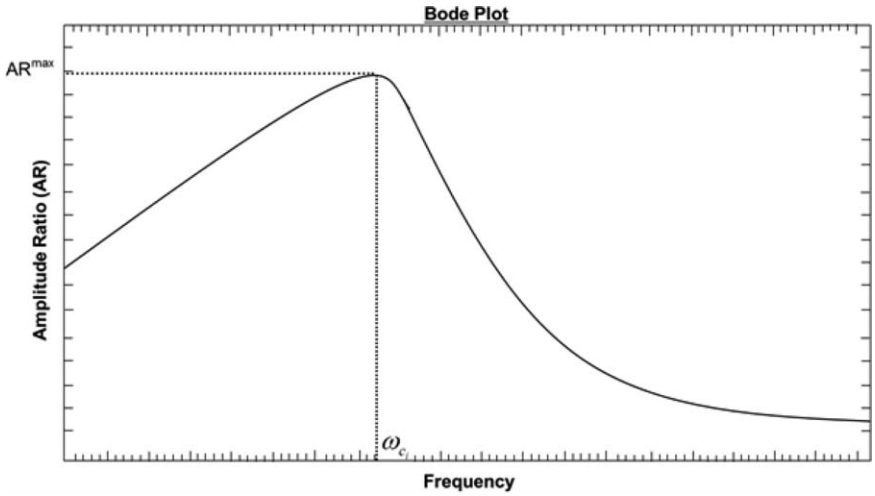

Figure 2. Bode plot, frequency response analysis.

The linearized closed-loop model (4) can further be represented in the frequency domain for each pair of k^{th} process disturbance and l^{th} controlled variable as follows

$$\mathbf{G}_{i,\mathbf{y}_l-\boldsymbol{\eta}_k}(j\omega)=\mathbf{C}_{i,\mathbf{y}_l-\boldsymbol{\eta}_k}(j\omega\mathbf{I}_{\mathbf{y}_l-\boldsymbol{\eta}_k}-\mathbf{A}_{i,\mathbf{y}_l-\boldsymbol{\eta}_k})^{-1}\mathbf{B}_{\mathbf{i},\mathbf{y}_l-\boldsymbol{\eta}_k}+\mathbf{D}_{\mathbf{i},\mathbf{y}_l-\boldsymbol{\eta}_k} \tag{5}$$

where j is the imaginary number ($j=\sqrt{-1}$), while ω denotes the frequency domain. $\mathbf{G}_{i,\mathbf{y}_l-\boldsymbol{\eta}_k}(j\omega)$ represents the transfer function between the k^{th} process disturbance and the l^{th} controlled variable. The matrices shown in (5) represent the dynamics between the k^{th} process disturbance and the l^{th} controlled variable and are subsets of the matrices shown in (4), that is, $\mathbf{A}_{i,\mathbf{y}_l-\boldsymbol{\eta}_k}\in\mathbf{A}_i$, $\mathbf{B}_{i,\mathbf{y}_l-\boldsymbol{\eta}_k}\in\mathbf{B}_i$, $\mathbf{C}_{i,\mathbf{y}_l-\boldsymbol{\eta}_k}\in\mathbf{C}_i$, $\mathbf{D}_{i,\mathbf{y}_l-\boldsymbol{\eta}_k}\in\mathbf{D}_i$

$\mathbf{G}_{i,\mathbf{y}_l-\boldsymbol{\eta}_k}(j\omega)$ can be further decomposed as follows

$$\mathbf{G}_{i,\mathbf{y}_l-\boldsymbol{\eta}_k}(j\omega)=R_{\mathbf{y}_l-\boldsymbol{\eta}_k}(\omega)+I^m_{\mathbf{y}_l-\boldsymbol{\eta}_k}(\omega)j \tag{6}$$

where $R_{\mathbf{y}_l-\boldsymbol{\eta}_k}(\omega)$ and $I^m_{\mathbf{y}_l-\boldsymbol{\eta}_k}(\omega)$ are the real and imaginary parts of the transfer function and are functions of the frequency ω. The amplitude ratio representing the variability in $\mathbf{y}_l$ due to changes in $\boldsymbol{\eta}_k$ can be expressed as follows

$$\mathrm{AR}_{\mathbf{y}_l-\boldsymbol{\eta}_k}=\sqrt{R_{\mathbf{y}_l-\boldsymbol{\eta}_k}(\omega)^2+I^m_{\mathbf{y}_l-\boldsymbol{\eta}_k}(\omega)^2} \tag{7}$$

From frequency response analysis, the maximum amplitude ratio, which corresponds to the maximum variability expected in $\mathbf{y}_l$ due to $\boldsymbol{\eta}_k$, is achieved at the critical frequency $\omega_{c_{k,i}}$. Following Eq. 7, the maximum amplitude ratio can be expressed as follows

$$\mathrm{AR}^{\max}_{\mathbf{y}_l-\boldsymbol{\eta}_k}=\sqrt{R_{\mathbf{y}_l-\boldsymbol{\eta}_k}(\omega_{c_{k,i}})^2+I^m_{\mathbf{y}_l-\boldsymbol{\eta}_k}(\omega_{c_{k,i}})^2} \tag{8}$$

The maximum amplitude ratio is pictorially represented in Figure 2 via Bode plot. As the amplitude ratio corresponding to the critical frequency is maximum, the disturbance generates the worst case variability in the controlled variable at this frequency. Note that for the cases where there is no clear maximum frequency (e.g., first-order system), that is, a range of frequencies correspond to maximum amplitude ratio in a bode plot, a numerical approximation must be made by selecting as critical frequency the highest or smallest frequency value that generates the maximum variability in the controlled variable.

Following Eq. 2, the critical frequency for each process disturbance k is specified for each grade i and for each critical scenario z as shown in (1) from the following equation

$$\boldsymbol{\eta}^z_k(t)=\boldsymbol{\eta}^z_{k_{\text{nom}}}+\boldsymbol{\eta}^z_{k_m}\sin(\omega^z_{c_{k,i}}t) \tag{9}$$

That is, the process disturbances are specified for each grade i using the critical frequency ($\omega_{c_{k,i}}$) that generates the maximum variability in the controlled variables at each critical realization z in the uncertain parameters $\mathbf{w}$.

For the cases where multiple disturbances are simultaneously acting on the controlled variables, the critical frequency at which the disturbances generate the maximum variability in a controlled variable is the frequency that produces the maximum total amplitude ratio. The total amplitude ratio is the sum of individual amplitude ratios for the disturbances.

Therefore, Eq. 8 can be modified for multiple disturbances as follows

$$\mathrm{AR}^{\max}_{\mathbf{y}_l-\boldsymbol{\eta}}=\sum_{k=1}^{K}\sqrt{R_{\mathbf{y}_l-\boldsymbol{\eta}_k}(\omega_{c,i})^2+I^m_{\mathbf{y}_l-\boldsymbol{\eta}_k}(\omega_{c,i})^2} \tag{10}$$

where K represents number of process disturbances acting simultaneously on l^{th} controlled variable, while $\omega_{c,i}$ represents the common critical frequency for the simultaneously acting disturbances that produces the maximum amplitude ratio in the l^{th} controlled variable.

Using these disturbances' critical frequency specifications, the worst-case variability is computed in the controlled variables through simulation of the closed loop nonlinear process model $\mathbf{f}_{\text{closed}}$ of the system for transition and production for all the grades. As mentioned above, the approach relies on the linear approximation of the nonlinear closed loop process model to identify the critical frequency for the process disturbances. Thus, the maximum (worst-case) variability in the controlled variables is the result of the linear approximation, which limits the approach from considering the true maximum variability of the nonlinear behavior. This particular aspect of the methodology will be examined using one of the case studies presented in this work.

Nominal closed-loop stability

Once a linear closed-loop model representation of the actual nonlinear closed-loop system is available, it can be used to evaluate the system's nominal stability under disturbances and uncertainty in the model parameters. The stability check can be conceptually formulated for each grade i and each critical scenario z of the uncertain parameter as follows

$$\mathrm{eig}(\mathbf{A}_i^z(\mathbf{x}_{\mathrm{lin}})|_{\mathbf{d}}) < \mathbf{0},\ \forall\, i=1\ldots I \tag{11}$$

where "eig" denotes the eigenvalues of linearized state matrices $\mathbf{A}_i^z$ at the operating point specified for grade i. Note that the $\mathbf{A}_i^z$ state space matrices include all the inputs and outputs considered in the linear state-space representation shown in (4) and they must be identified at each optimization step, that is, around the set of values specified for the methodology's optimization variables $\mathbf{d}$. Constraint (11) will, therefore, be added to the methodology's optimization formulation to enforce nominal stability for the different operating points that need to be achieved by the system to produce the required grades.

Cost function

The cost function $\varnothing$ considered in the presented methodology includes the capital cost, operating cost, variability cost, and transition cost. The annualized capital costs (CC) refers to the fixed costs/capital investments associated with the process equipment and units in the process and is given by the following equation

$$\mathrm{CC}=f(V_E,W_E,Z_E)+\sum_{i=1}^{I} f(V_i,W_P,Z_P) \tag{12}$$

where V_E is the size of the process equipment and W_E is the annual capital recovery factor per unit size of equipment; V_i represents the size of the storage tank used to store product grade i whereas W_P is the annual capital recovery factor per unit size of that product storage tank. Z_E and Z_P denote the per unit capital costs associated with the equipment and product tanks. The volume of the product tank is considered to be a measure of the variability in the product grade specification, that is, with higher product variability due to disturbances and model parameter uncertainty, more off-specification product is produced which leads to larger volumes of the product tanks thus affecting the plant's economy.

The operating cost OC represents the expenditure associated with production in terms of consumption of utilities; this cost can be calculated from the per unit rates for utilities. The variability cost VC aims to measure the effect of time-varying disturbances and model parameter uncertainty during the production stage, that is, product variability. As shown in Figure 3a, the minimum and maximum values around the set point for specification of a grade i can be used to calculate the variability cost as follows

$$\mathrm{VC}=\sum_{i=1}^{I} t_{p_i}((\mathrm{Max}C_i(t)-C_i^{\mathrm{SP}})+(C_i^{\mathrm{SP}}-\mathrm{Min}C_i(t)))P_{V,i}/t_{\mathrm{total}} \tag{13}$$

where t_{p_i} is the production time required for grade i, t_{total} is the total time of production cycle, C_i^{SP} denotes the specification for product grade i, while $\mathrm{Max}C_i(t)$ and $\mathrm{Min}C_i(t)$ are the maximum and minimum values associated with the specification at any time t within the production time interval for the grade i, that is, t_{pi}. Both $\mathrm{Max}C_i(t)$ and $\mathrm{Min}C_i(t)$ are obtained from simulations of the nonlinear closed loop process model $\mathbf{f}_{\mathrm{closed}}$ for the production stages of grade i. The term $P_{V,i}$ is a user-defined penalty cost associated with product variability of grade i per unit time. Furthermore, the transition cost TC represents the cost associated with the waste production during the transition from one grade to another, which is off-specification.

The deviations ($\varepsilon(t)$) between the set-point associated with the grade specification (C_i^{SP}) and the actual grade at time t ($C_i(t)$) are shown in Figure 3b, which are used to calculate the transition cost. The deviations $\varepsilon(t)$ are evaluated at discrete time intervals over transition period t_i. The time is discretized in N intervals and sum of squared errors is evaluated as follows

$$\mathrm{SSE}_i=\sum_{n=0}^{N}\varepsilon(n\Delta t)^2,\ \ \forall t=0,\Delta t,2\Delta t,3\Delta t....n\Delta t...N\Delta t \tag{14}$$

where Δt is the sampling time at which deviations are evaluated, while $N\Delta t$ represents the total integration time, that is, transition period t_i. Accordingly, the transition cost can be estimated as follows

$$\mathrm{TC}=\sum_{i=1}^{I} P_{T,i}t_i\mathrm{SSE}_i/t_{\mathrm{total}} \tag{15}$$

where t_i is the transition time for the grade i and $P_{T,i}$ is the user-defined penalty during the transition stage from grade $i-1$ to grade i, which is the cost associated with the production of the off-specification product of grade i per unit time.

Optimization formulation

Following the developments in the previous subsections, an MINLP optimization formulation to address the simultaneous design, scheduling, and control can be formulated for multiproduct process that produces I number of grades of product under the influence of process disturbances ($\boldsymbol{\eta}$) and model parameter uncertainty ($\mathbf{w}$)

$$\begin{gathered}
\min_{\mathbf{d}=[\boldsymbol{\kappa},\boldsymbol{\Lambda},\mathbf{S}]} \varnothing=\sum_{z=1}^{\mathrm{ns}} P^z(CC+OC+VC+TC)\\
\text{s.t.}\\
\mathbf{f}(\mathbf{x}^z(t),\dot{\mathbf{x}}^z(t),\mathbf{u}^z(t),\boldsymbol{\eta}^z(t),\mathbf{y}^z(t),\boldsymbol{\theta}^z(t),\boldsymbol{\kappa},\mathbf{w}^z(t))=0,\ z=1\,..\,\mathrm{ns}\\
\mathbf{g}(\mathbf{x}^z(t),\dot{\mathbf{x}}^z(t),\mathbf{c}^z(t),\dot{\mathbf{c}}^z(t),\mathbf{u}^z(t),\mathbf{y}^z(t),\mathbf{w}^z(t),\boldsymbol{\Lambda})=0\,,\ \ z=1\,..\,\mathrm{ns}\\
\mathbf{h}\,(\mathbf{x}^z(t),\mathbf{u}^z(t),\boldsymbol{\eta}^z(t),\mathbf{y}^z(t),\boldsymbol{\theta}^z(t),\boldsymbol{\kappa},\boldsymbol{\Lambda},\mathbf{S},\mathbf{w}^z(t))=0\,,\ z=1\,..\,\mathrm{ns}\\
\dot{\mathbf{x}}_{\mathrm{lin}}^z=\mathbf{A}_i^z\mathbf{x}+\mathbf{B}_i^z\boldsymbol{\varphi}\\
\boldsymbol{\Omega}_{\mathrm{lin}}^z=\mathbf{C}_i^z\mathbf{x}+\mathbf{D}_i^z\boldsymbol{\varphi},\ \ i=1...I\,,\ z=1\,..\,\mathrm{ns}\\
\mathrm{eig}(\mathbf{A}_i^z(\mathbf{x}_{\mathrm{lin}})_{\mathbf{d}})<0\,,\ \forall i=1....n\,,\ \ z=1\,..\,\mathrm{ns}\\
\boldsymbol{\eta}_k^z(t)=\boldsymbol{\eta}_{k_{\mathrm{nom}}}^z+\boldsymbol{\eta}_{k_m}^z\sin\left(\boldsymbol{\omega}_{\mathbf{c}_{k,i}}^z t\right)\,,\ i=1\,....\,n\,,\ z=1..\mathrm{ns},\forall k\\
\mathbf{d}^l\le\mathbf{d}\le\mathbf{d}^u
\end{gathered} \tag{16}$$

where the decision variables ($\mathbf{d}$) consist of process design variables $\boldsymbol{\kappa}$, tuning parameters for the control scheme considered $\boldsymbol{\Lambda}$ and the scheduling parameters $\mathbf{S}$. The design variables ($\boldsymbol{\kappa}$) consist of fixed/equipment design parameters and

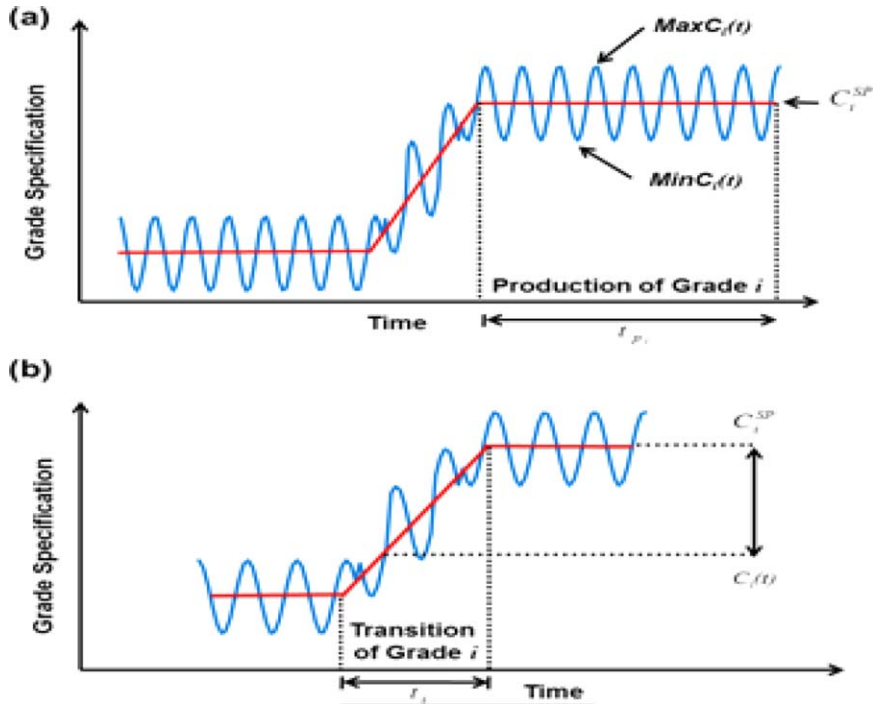

Figure 3. Assessing the costs: (a) variability cost; (b) transition cost.

[Color figure can be viewed in the online issue, which is available at wileyonlinelibrary.com.]

nominal operating conditions for each grade i, that is, ($\overline{\mathbf{u_i}}$ and $\overline{\mathbf{y_i}}$), while the scheduling parameters ($\mathbf{S}$) involve the optimal sequence of production $\mathbf{s}$, which is a set of integer variables, that is, $\mathbf{s} \in \mathbf{Z}^{Ix1}$, and the set of transition slopes for each grade i, $\boldsymbol{\alpha} \in \mathbf{R}^{Ix1}$. The slope for the transition for a grade i is defined as follows

$$\alpha_i = \frac{C_i^{\mathrm{SP}} - C_{i-1}^{\mathrm{SP}}}{t_i} \tag{17}$$

where t_i is the transition time for grade i whereas C_i^{SP} and C_{i-1}^{SP} represent the product grade specifications for grades i and $i-1$, respectively (see Figure 1). The remaining variables used in (16) are listed under in the notation section. The optimization formulation shown in (16) involves the use of linearized closed-loop model, frequency response analysis, nominal stability check via eigenvalues, and dynamic simulations of the actual process model in closed-loop under critical realizations in the disturbances and for each uncertain (discrete) scenario considered in the analysis. Given, an initial set of values in the decision variables $\mathbf{d}_0$, an nonlinear process model ($\mathbf{f}$), closed-loop control scheme ($\mathbf{g}$), nominal values ($\boldsymbol{\eta}_{\mathrm{nom}}$) and amplitudes ($\boldsymbol{\eta}_m$) for disturbances, product grade specifications (C_i^{SP}) and demands (V_{p_i}) and critical scenarios for uncertain parameters ($\mathbf{w}$), the following steps are followed at each optimization step to evaluate the cost function and constraints included in problem (16):

1. For each grade i, the linearized closed loop model of the system is identified for each critical realization in uncertain parameters by linearization of nonlinear closed-loop model $\mathbf{f}_{\mathrm{closed}}$ at the nominal operating steady-state conditions specified by decision variables $\mathbf{d}$. The linearized closed-loop model will be used to identify the critical frequencies in the process disturbances that are expected to generate the largest variability in the production stage of grade i, that is, $\omega_{c_{k,i}}$.

2. For each grade i, the critical frequency ($\omega_{c_{k,i}}$) is identified from the linearized model for each critical realization in uncertain parameters via frequency response analysis as described by Eqs. 2–9. The disturbances are specified using the critical frequency and model parameter uncertainty scenarios as shown in (9).

3. For each grade i and each critical realization in the uncertain parameter w^z, a stability check is performed for the nominal stability of the system via evaluation of the eigenvalues as shown in (11).

4. For each critical scenario in the uncertainty in the parameters, the transition and production for all the grades is achieved through simulation of the closed loop nonlinear process model $\mathbf{f}_{\mathrm{closed}}$ of the system. This is achieved under the influence of critical realizations in the disturbances using ($\omega_{c_{k,i}}$) and that were identified from step 2 for each grade i.

5. The simulation results from the previous step are then used to evaluate the process constraints and each of the cost function terms described above. If an optimization criterion is met, the optimization algorithm stops, else it leaves the workflow and the steps are repeated with new set of decision variables, that is, go back to step 1.

Remarks

The methodology presented in this work integrates the design, scheduling, and control aspects of the multiproduct plants under the influence of process disturbances and uncertainty in the parameters. These aspects are novel features introduced by the present study as they have never been considered before for the optimal design of multiproduct plants. The process disturbances ($\boldsymbol{\eta}$) are specified as sinusoidal functions at critical frequency obtained from the linearized closed-loop process model. This variability may not be the true worst-case as the responses for controlled variables are linearized. While the actual critical frequency that generates

the worst-case variability in the controlled variables can be obtained from a formal dynamic feasibility analysis test,[28,41,44] this test needs to be performed for each grade i and at each optimization step thus increasing the computational costs and may even becoming prohibitive if the problem under analysis is relatively large. The approach proposed here is expected to provide reasonable accurate results as the critical frequency is identified under feedback control. As such, it is expected that the control actions will aim to maintain the system around a nominal operating point (i.e., the product grade's set-point) thus making the linear closed-loop approximation valid. Tests need to be performed to evaluate this approximation. Furthermore, the approach of computing critical frequency corresponding to worst case variability can be assumed when there is no prior information available for the anticipated range of frequencies of the disturbances. However, there are cases where the optimal process design needs to be specified at a particular frequency range for the disturbances, which is known to be harmful for the process or that is continuously affecting the process during its normal operation. For the cases where this information is available *a priori*, the anticipated range of frequencies for the disturbances can be used instead of the critical frequency in order to attenuate most of the typical (or harmful) anticipated disturbances at a given (prespecified) frequency range. This may provide more realistic (less conservative) process designs. Accordingly, Eq. 8 can be modified to represent this range of frequencies that correspond to anticipated disturbances as follows

$$\mathrm{AR}^{\max}_{\mathbf{y}_l-\boldsymbol{\eta}_k}=\sqrt{R_{\mathbf{y}_l-\boldsymbol{\eta}_k}(\omega_{c_{k,i}})^2+I^m_{\mathbf{y}_l-\boldsymbol{\eta}_k}(\omega_{c_{k,i}})^2},\quad \omega_l\le\omega_{c_{k,i}}\le\omega_u \tag{18}$$

That is, the search for the maximum amplitude ratio that produces the largest variability in the l^{th} controlled variable is limited to a particular frequency range for the disturbances at which the optimal design, scheduling, and control will be performed. The limits ω_l and ω_u represent the lower and upper bounds on the frequencies which represent the anticipated range of frequencies for the process disturbances that have been prespecified *a priori* by the user.

Moreover, the process flow sheet of the multiproduct process has been assumed to remain the same throughout the calculations in the presented methodology. The control scheme has also been assumed to be fixed. This leads the methodology to be able to compute the process scheduling, design, and control parameters only for the fixed flow sheet and control structures. To make the methodology robust to the changes in the flow sheet and control schemes, advanced approaches need to be considered which result in higher computational costs. The application of such highly demanding approaches to the methodology of integration of scheduling, design, and control is considered part of the future work in this study. In terms of product grades, the production of all the grades has been assumed to be consumed/sold before the production begins, that is, availability of storage tanks has been assumed to be constant. All grades are produced only once in the complete operation cycle.

Results and Discussions

This section describes the two case studies developed for the application of the methodology described in this study. The two applications demonstrate the effect of simultaneous consideration of the three aspects on the overall cost of operation, that is, design, control, and scheduling. The results presented for these case studies were obtained using MATLAB software on system with a Win Server 2012, Intel® Core i7-3770 CPU 340GHz, 8 GB RAM.

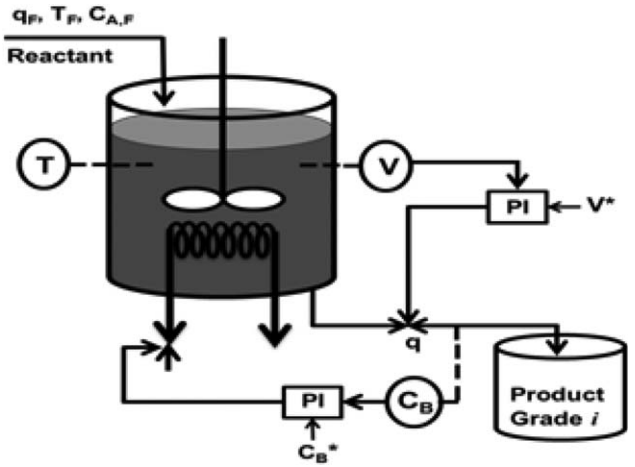

Figure 4. Nonisothermal CSTR system.

Case study 1: Nonisothermal CSTR

The methodology discussed in the previous section has been applied to a nonisothermal CSTR system with an irreversible reaction which is assumed to produce three grades of the product. Figure 4 shows the CSTR system pictorially with a reactor, control system, and product tanks for the three grades to be produced which are to be filled one by one. However, the sequence of filling the tanks, that is, the production of grades, is part of the decision variables. The case study has been developed to simultaneously determine the optimal design, control, and scheduling parameters for the CSTR system under consideration, compare the results against the semisequential approach, that is, optimal design and control followed by optimal scheduling, and evaluate the methodology's capability to handle uncertainty in grade demands.

Mathematical Model. An irreversible exothermic reaction $\mathrm{A}\rightarrow\mathrm{B}$ occurs in the CSTR for the production of product B from reactant A. The reaction has been assumed to follow first-order dynamics and the reaction rate is given by the Arrhenius law as follows

$$r_{\mathrm{A}}=k_0C_{\mathrm{A}}\ \exp\left(-\frac{E}{RT}\right) \tag{19}$$

where C_{A} (mol/L) is the concentration of reactant A inside the reactor at any time t, k_0 is the pre-exponential factor (7.2 e −10), E is the activation energy (8.3145 J/mol), and R is the gas constant (8.3144 J/mol K). The CSTR system is equipped with a cooling jacket in order to maintain the temperature inside the reactor (T). The concentration of reactant A in the inlet stream ($C_{\mathrm{A},F}$) has been assumed to remain constant during the operation ($C_{\mathrm{A},F}=2\,\mathrm{mol/L}$). The mechanistic dynamic model that describes the nonisothermal CSTR system is given as follows

$$\frac{dV}{dt}=q_F-q \tag{20}$$

$$\frac{dT}{dt}=\frac{q_F(T_F-T)}{V}+\frac{(H_0k_0\exp(\frac{-E}{RT})(C_{A,F}-C_B)}{\rho C_p}-Q_C(C_B^*-C_B) \tag{21}$$

$$\frac{dC_B}{dt}=k_0\exp\left(-\frac{E}{RT}\right)(C_{A,F}-C_B)-\frac{C_Bq}{V} \tag{22}$$

$$q=10u_2\sqrt{V} \tag{23}$$

$$Q_C=48.1909\ u_1 \tag{24}$$

where the volume of the reactor (V), the temperature inside the reactor (T), and the product concentration (C_B) are the states and outputs of the system. As shown in (23) and (24), the outlet flow rate of the reactor q is used to control the volume (V) or level in the reactor, while the heat flow to the system (Q_C) has been used as a handle to control the amount of heat transferred to the CSTR system, respectively. There are two manipulated variables available in the system, that is, u_1 and u_2 $(\mathbf{u}=[u_1,u_2])$. The two manipulated variables are used to control the volume of the reactor (V) and the product concentration (C_B), respectively. The density of the fluid is ρ (1e3 g/L), C_p is the fluid's heat capacity (0.239 J/g K), while H_0 is the heat of reaction (4.78e4 J/mol).

Two proportional and integral (PI) controllers have been used to regulate this process. K_{C_1} and K_{C_2} represent the two controller gains whereas τ_1 and τ_2 are the time integral time constants for the two controllers, that is, tuning parameters $(\mathbf{\Lambda}=[K_{C_1},K_{C_2},\tau_1,\tau_2])$. The errors e_1 and e_2 for the two controllers at any time t represent the difference between the set-points (V^* and C_B^*) and the controlled variables' values at time t, that is, $V(t)$ and $C_B(t)$. The aim of the irreversible reaction is to produce required grades of product B. Each grade is characterized with specification in terms of product concentration $(C_{B_i}^*)$ and a demand in terms of product volume (V_{p_i}). As shown in Figure 4, the system consists of a reaction vessel and a dedicated product tank for each grade of product. The dynamics of the product tank for grade i of product B can be represented by the following equation

$$\frac{dV_{P_i}}{dt}=q \tag{25}$$

The product tank for a particular grade starts filling as soon as required product specification of a grade is achieved, that is, production period for grade i starts. The time at which the condition is satisfied gives the transition time required for the grade i, that is, t_i. The product tank continues filling until the required product demand is achieved and specification has been maintained. The product tank is then instantaneously changed to the product tank for the next required grade of the product. The time at which this happens is the production time of the grade i.

The following operational constraint has been applied to impose limits on the temperature of the CSTR

$$430\le T(t)\le 500 \tag{26}$$

Process Disturbances. Following the disturbance description shown in (2), the process disturbances T_F and q_F are defined as follows

$$\begin{aligned}T_F(t)&=450+10\sin(\omega_{c_{T_F,i}}t)\\ q_F(t)&=200+10\sin(\omega_{c_{q_F,i}}t)\end{aligned} \tag{27}$$

For each grade i, the critical frequencies $(\omega_{c_{T_F,i}},\omega_{c_{q_F,i}})$ used to generate the disturbances are obtained from the frequency response analysis of linearized closed-loop process model at operating conditions for each grade i specified by the decision variables **d**.

Cost Function. The annualized capital cost of the CSTR system associated with the volume of the reactor and the volume of the product grade tanks can be formulated as follows

$$\mathrm{CC}=1000(0.1)V+\sum_{i=1}^{I}1000(0.1)V_{p_i} \tag{28}$$

where V is the volume for the reactor whereas V_{p_i} is the volume of product tank for grade i. To simplify the analysis, all costs associate with the equipment have been assigned the same value. Following (12), $W=0.1/\mathrm{year}$, $Z=\$1000$, $W_P=0.1/\mathrm{year}$, and $Z_P=\$1000$.

Moreover, the variability cost can be calculated by modifying (13) as follows

$$\mathrm{VC}=\sum_{i=1}^{I}t_{p_i}((\mathrm{Max}C_{B_i}(t)-C_{B_i}^*)+(C_{B_i}^*-\mathrm{Min}C_{B_i}(t)))10/t_{\mathrm{total}} \tag{29}$$

where $C_{B_i}^*$ is the product grade specification, $C_{B_i}(t)$ is the value at time t for the product concentration, while the penalty for variability has been assigned the value of \$10/(mol/L) min.

The operating cost can be calculated as follows

$$\mathrm{OC}=\sum_{i=1}^{I}t_{p_i}(10(\overline{Q_{c_i}}))/t_{\mathrm{total}} \tag{30}$$

where $\overline{Q_{c_i}}$ is the steady-state value for heat duty at production of each grade i, while 10 is the per unit cost of heat per unit time.

Furthermore, the transition cost can be calculated from (15) as follows, that is,

$$\mathrm{TC}=\sum_{i=1}^{I}10t_i\mathrm{SSE}_i/t_{\mathrm{total}} \tag{31}$$

where SSE_i is the sum of squared errors during the transition period of the grade i as shown in (14). The penalty for waste production has been assigned the value of $\$10/(\mathrm{mol/L})^2$ min.

Following the developments above, the optimization formulation has been solved for the CSTR system. The decision variables to be evaluated include volume of the reactor and steady-state operating conditions for each grade $(\boldsymbol{\kappa}=[V,\overline{u_{1i}},\overline{u_{2i}}\ ])$, tuning parameters for the two PI controllers $(\mathbf{\Lambda}=[K_{C_1},K_{C_2},\tau_1,\tau_2])$, slopes for transition of each grade, that is, $\alpha_1,\alpha_2,\alpha_3$, and the optimal sequence of production (**s**).

Scenario 1. This scenario has been developed to compare the results obtained via the present simultaneous approach and a semisequential approach. In the semisequential approach, the following procedure was considered: in the first step, decision variables related to process design and control (i.e., integration of design and control) are evaluated first and then in the second step, the scheduling decision variables are determined while the design and control variables obtained in step 1 remain fixed in the calculations. The specifications and the demands of the required product grades

Table 1. Grade Specifications, Demands, and Results for Scenario 1, Case Study CSTR

Grade Specifications and Demands		
Grade	Product Concentration (mol/L)	Demand (L)
1	1.7023	3,000
2	1.830	3,000
3	1.950	3,000

Results		
Decision Variables and Costs	Simultaneous Approach	Semisequential Approach
Design		
V (L)	80.6828	87.416
Control:		
$K_{C_1}, K_{C_2}, \tau_1, \tau_2$	−13.634, −0.002, 7.40, 8.77	−5.425, −0.0016, 2.235, 9.314
Scheduling:		
s (sequence of grades)	2-1-3	2-1-3
$\alpha_1, \alpha_2, \alpha_3$ (transition slopes)	0.0872, −0.0803, 0.006	0.0131, −0.0281, 0.0011
Capital Cost ($/year)	15,716	18,844
Operating Cost ($/year)	1021	1699
Variability Cost ($/year)	132	319
Transition Cost ($/year)	153	382
Total Cost ($/year)	17,021	21,244

considered for the problem addressed for this scenario are reported in Table 1.

The methodology has been used to obtain results for the CSTR system to integrate the scheduling, design, and control aspects of the system. For each single function evaluation, values for the decision variables are selected by the optimization algorithm. These decision variables are further used to calculate for each grade i, steady-state operating conditions ($\overline{u_{1i}}$, $\overline{u_{2i}}$, T_i) by solving the process model (**f**) at steady state. For each grade i, the steady-state operating conditions are then used to identify a linear closed-loop model of the system as shown in (4). The resulting linear model is further used to identify the critical frequency ($\omega_{c_{k,i}}$) for each grade i for each process disturbance (T_F, q_F) as described by Eqs. 2–9, which is used to specify the process disturbances as shown in (2). The closed-loop process model described by Eqs. 19–25 is simulated for each critical scenario for uncertainty in product demand. The results from this simulation are then used to evaluate the process constraints and cost function shown in (16). This procedure is repeated until an optimization criterion is met.

The results obtained from the implementation of the two approaches are reported in Table 1 (Results). The decision variables obtained from each approach vary significantly from each other and there is approximately 20% improvement in the overall cost with the simultaneous approach as compared to the semisequential approach. The maximum improvement can be seen in the transition costs (~60%). The volume of the reactor (V), which is a design decision variable, is almost 8% less in the simultaneous approach than that obtained in semisequential approach, while tuning parameters for the two controller are also significantly different, which indicates that different process performance may be obtained from the two solution methods.

The slopes obtained for the transition between the grades of the product are observed to be more aggressive in simultaneous approach as compared to semisequential approach, which provide the basis for the improvement in the transition cost. The transition and production of various grades are depicted in Figure 5a. The variability in the concentration is the result of process disturbances oscillating at critical

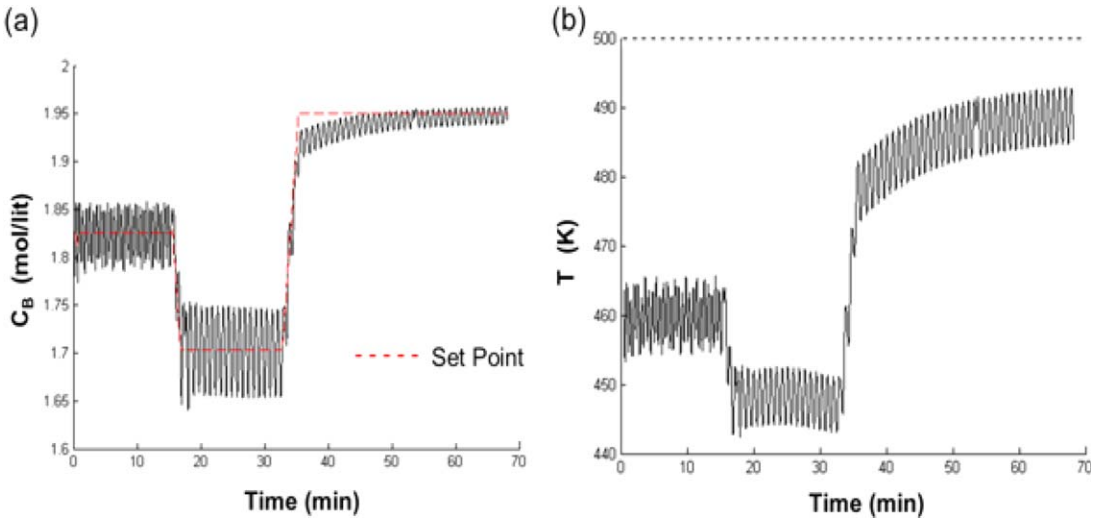

Figure 5. CSTR case study, scenario 1: (a) transition and production of product grades; (b) temperature profile.

[Color figure can be viewed in the online issue, which is available at wileyonlinelibrary.com.]

Table 2. Demands and Probabilities of Scenarios, CSTR

Demand Scenario	Demands of Product Grades: 1, 2, 3 (L)	Probability
1	3000, 3000, 3000	0.4
2	5000, 2000, 1000	0.3
3	2000, 5000, 1000	0.2
4	1000, 5000, 2000	0.1

Results	
Decision Variables and Costs	Values
Design:	
V (L)	75.655
Control:	
$K_{C_1}, K_{C_2}, \tau_1, \tau_2$	−16.4633, −0.073, 3.6428, 10.0432
Scheduling:	
s (sequence of grades)	2-1-3
$\alpha_1, \alpha_2, \alpha_3$ (transition slopes)	0.0507, −0.510, 0.00265
Total Cost ($/year)	17,206

frequency, which has a different value for each grade obtained via frequency response analysis of linearized process model at the different operating conditions specified by **d**. Although the critical frequency in inlet flowrate and the inlet temperature that produced the worst-case variability in the reactor's concentration turned out to be at a frequency that is higher than normal frequency to that typically observed for changes in concentration, the present analysis was performed under the worst-case scenario assumption. However, as described in Remarks section, the present methodology can be easily adapted to perform this analysis at a given (prespecified) frequency range for the disturbances that is known to occur frequently during normal operation or that are particularly harmful for the process. The process constraint on temperature has been satisfied throughout the operation of the entire production cycle as shown in Figure 5b. Thus, the results obtained via two approaches show that the simultaneous methodology generates more economical solution as compared to the semisequential approach.

Scenario 2. This second scenario has been developed to evaluate the capability of the methodology developed in this study to handle uncertainty in the parameters. As shown in the methodology's formulation in (16), a multiscenario approach has been used for this purpose; critical scenarios have been created with a specific demand for each grade of the product. Each scenario has been assigned the probability of occurrence of the scenario. As shown in Table 2, four demand scenarios have been created with first scenario with uniform production demands, that is, 3000 L of each grade having the highest probability of occurrence. The other three scenarios consist of maximum and minimum of the demands for each grade of the product.

The optimization formulation presented in (16) has been modified for this scenario and the results obtained are also shown in Table 2 (Results). As shown in this table, the optimal volume of the reactor is 75.655 L, while the optimal sequence of production is determined to be 2-1-3, which is same as in Scenario 1, that is, without uncertainty in demands. Figure 6 depicts the trends for transition and production of the grades in four critical scenarios for uncertainty in demands, where optimal smooth transitions between grades is the result of optimal transition slopes computed by the optimization formulation. This is achieved while maintaining the dynamic operability of this process under their corresponding constraints (not shown here for brevity).

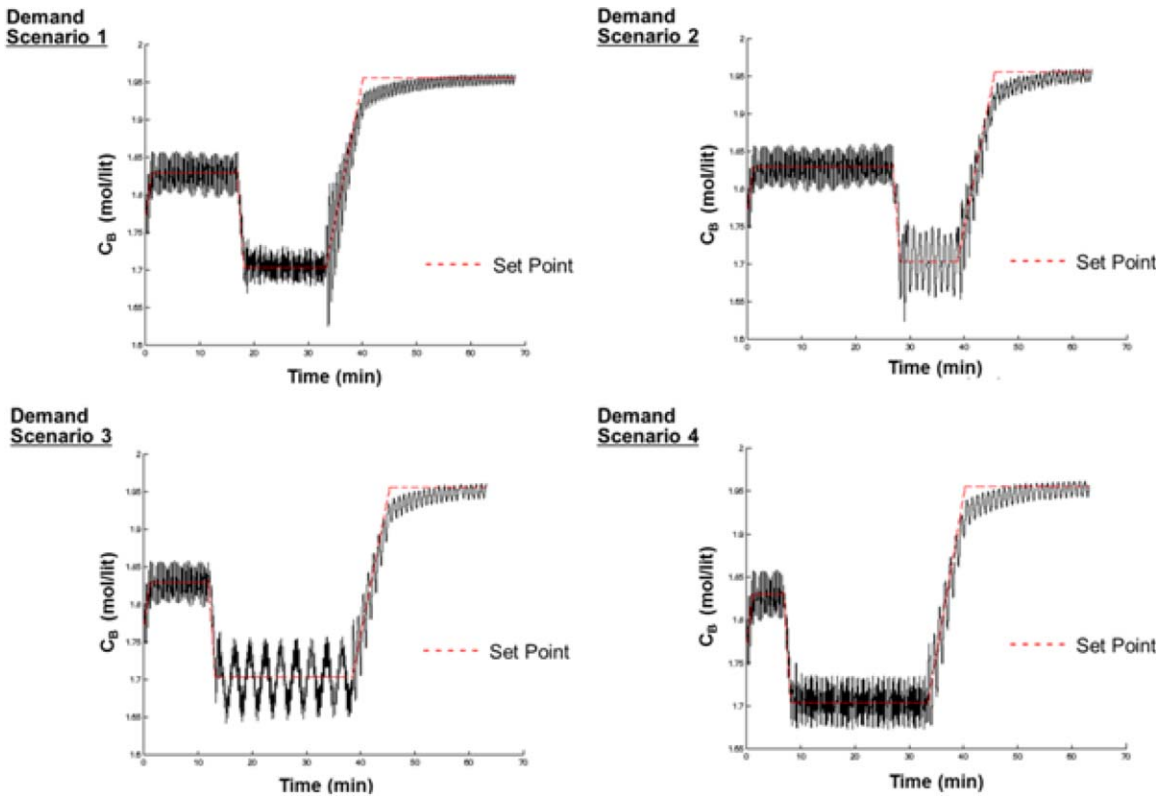

Figure 6. CSTR case study, scenario 2: transition and production of product grades under uncertainty in demands.

[Color figure can be viewed in the online issue, which is available at wileyonlinelibrary.com.]

In terms of computational costs, the computational time required to complete a single evaluation of the optimization formulation for Scenario 1 was 40 s on average, while the solution was obtained in 2.5 h. For Scenario 2, the single evaluation of the optimization formulation required 60 s on average, while the solution was obtained in 3 h.

Case study 2: HIPS polymerization reactor

The second case study has been developed with the goal of demonstrating the capability of the methodology to be applied to a large-scale problem with a high nonlinear behavior. While several large-scale applications in process scheduling have been reported in the literature,[70–72] the implementation of simultaneous design, scheduling, and control methodologies to large-scale chemical systems is limited. The present case study focusses on integration of scheduling, design, and control aspects for the HIPS process characterized by the parameters and the mathematical model.[23] The process is operated by the continuous stirred tank reactor with highly nonlinear reaction mechanism. The results are obtained for the critical uncertain scenarios developed for the varying product demands.

Mathematical Model. Initiator Concentration

$$\frac{dC_{\mathrm{i}}}{dt}=\frac{q_{\mathrm{i}}C_{\mathrm{i}}^{\mathrm{in}}-q_{\mathrm{m}}C_{\mathrm{i}}}{V}-K_{\mathrm{d}}C_{\mathrm{i}} \tag{32}$$

Monomer Concentration

$$\frac{dC_{\mathrm{m}}}{dt}=\frac{q_{\mathrm{m}}(C_{\mathrm{m}}^{\mathrm{in}}-C_{\mathrm{m}})}{V}-K_P C_{\mathrm{m}}(\varepsilon_{\mathrm{r}}^0+\varepsilon_b^0) \tag{33}$$

Butadiene Concentration

$$\frac{dC_{\mathrm{b}}}{dt}=\frac{q_{\mathrm{m}}(C_{\mathrm{b}}^{\mathrm{in}}-C_{\mathrm{b}})}{V}-C_{\mathrm{b}}(K_{\mathrm{i}2}C_{\mathrm{r}}+K_{\mathrm{fs}}\varepsilon_{\mathrm{r}}^0+K_{\mathrm{fb}}\varepsilon_{\mathrm{b}}^0) \tag{34}$$

Radicals Concentration

$$\frac{dC_{\mathrm{r}}}{dt}=\frac{-q_{\mathrm{m}}}{V}C_{\mathrm{r}}+2e_{\mathrm{f}}K_{\mathrm{d}}C_{\mathrm{i}}-C_{\mathrm{r}}(K_{\mathrm{i}1}C_{\mathrm{m}}+K_{\mathrm{i}2}C_{\mathrm{b}}) \tag{35}$$

Branched radicals concentration

$$\begin{aligned}\frac{dC_{\mathrm{br}}}{dt}=&\frac{-q_{\mathrm{m}}}{V}C_{\mathrm{br}}+C_{\mathrm{b}}(K_{\mathrm{i}2}C_{\mathrm{r}}+K_{\mathrm{fb}}(\varepsilon_{\mathrm{r}}^0+\varepsilon_{\mathrm{b}}^0))\\&-C_{\mathrm{br}}(K_{\mathrm{i}3}C_{\mathrm{m}}+K_{\mathrm{t}}(\varepsilon_{\mathrm{r}}^0+\varepsilon_{\mathrm{b}}^0+C_{\mathrm{br}}))\end{aligned} \tag{36}$$

Reactor temperature

$$\frac{dT}{dt}=\frac{q_{\mathrm{m}}}{V}(T^{\mathrm{in}}-T)+\frac{\Delta H_{\mathrm{r}}K_{\mathrm{p}}C_{\mathrm{m}}(\varepsilon_{\mathrm{r}}^0+\varepsilon_{\mathrm{b}}^0)}{\rho_{\mathrm{st}}C_{\mathrm{ps}}}-\frac{UA(T-T_{\mathrm{j}})}{\rho_{\mathrm{st}}C_{\mathrm{ps}}V} \tag{37}$$

Jacket Temperature

$$\frac{dT_{\mathrm{j}}}{dt}=\frac{q_{\mathrm{cw}}}{V_c}(T_{\mathrm{j}}^{\mathrm{in}}-T_{\mathrm{j}})+\frac{UA(T-T_{\mathrm{j}})}{\rho_{\mathrm{st}}C_{\mathrm{ps}}V_c} \tag{38}$$

Zeroth moment live polymer

$$\frac{d\xi_{\mathrm{p}}^0}{dt}=\frac{-q_{\mathrm{m}}}{V}\xi_{\mathrm{p}}^0+\frac{K_{\mathrm{t}}}{2}(\varepsilon_{\mathrm{r}}^0)^2+(K_{\mathrm{fs}}C_{\mathrm{m}}+K_{\mathrm{fb}}C_{\mathrm{b}})\varepsilon_{\mathrm{r}}^0 \tag{39}$$

First moment live polymer

$$\frac{d\xi_{\mathrm{p}}^1}{dt}=\frac{-q_{\mathrm{m}}}{V}\xi_{\mathrm{p}}^1+K_{\mathrm{t}}\varepsilon_{\mathrm{r}}^1\varepsilon_{\mathrm{r}}^0+(K_{\mathrm{fs}}C_{\mathrm{m}}+K_{\mathrm{fb}}C_{\mathrm{b}})\varepsilon_{\mathrm{r}}^1 \tag{40}$$

Zeroth moment dead polymer

$$\begin{aligned}\frac{d\varepsilon_{\mathrm{r}}^0}{dt}=&\frac{-q_{\mathrm{m}}}{V}\varepsilon_{\mathrm{r}}^0+2K_{\mathrm{i}0}C_{\mathrm{m}}^3+2K_{\mathrm{i}1}C_{\mathrm{r}}C_{\mathrm{m}}+C_{\mathrm{m}}K_{\mathrm{fs}}(\varepsilon_{\mathrm{r}}^0+\varepsilon_{\mathrm{b}}^0)\\&-(K_{\mathrm{p}}C_{\mathrm{m}}+K_{\mathrm{t}}(\varepsilon_{\mathrm{r}}^0+\varepsilon_{\mathrm{b}}^0+C_{\mathrm{br}})+C_{\mathrm{m}}K_{\mathrm{fs}}+C_{\mathrm{b}}K_{\mathrm{fb}})\varepsilon_{\mathrm{r}}^0+K_{\mathrm{p}}C_{\mathrm{m}}\varepsilon_{\mathrm{r}}^0\end{aligned} \tag{41}$$

First moment dead polymer

$$\begin{aligned}\frac{d\varepsilon_{\mathrm{r}}^1}{dt}=&\frac{-q_{\mathrm{m}}}{V}\varepsilon_{\mathrm{r}}^1-(K_{\mathrm{p}}C_{\mathrm{m}}+K_{\mathrm{t}}(\varepsilon_{\mathrm{r}}^0+\varepsilon_{\mathrm{b}}^0+C_{\mathrm{br}})+C_{\mathrm{m}}K_{\mathrm{fs}}+C_{\mathrm{b}}K_{\mathrm{fb}})\\&\varepsilon_{\mathrm{r}}^0+K_{\mathrm{p}}C_{\mathrm{m}}(\varepsilon_{\mathrm{r}}^0+\varepsilon_{\mathrm{r}}^0)\end{aligned} \tag{42}$$

Zeroth moment butadiene

$$\begin{aligned}\frac{d\varepsilon_{\mathrm{b}}^0}{dt}=&\frac{-q_{\mathrm{m}}}{V}\varepsilon_{\mathrm{b}}^0+2K_{\mathrm{i}3}C_{\mathrm{br}}C_{\mathrm{m}}-(K_{\mathrm{p}}C_{\mathrm{m}}+K_{\mathrm{t}}(\varepsilon_{\mathrm{r}}^0+\varepsilon_{\mathrm{b}}^0+C_{\mathrm{br}})\\&+C_{\mathrm{m}}K_{\mathrm{fs}}+C_{\mathrm{b}}K_{\mathrm{fb}})\varepsilon_{\mathrm{b}}^0+K_{\mathrm{p}}C_{\mathrm{m}}\varepsilon_{\mathrm{b}}^0\end{aligned} \tag{43}$$

Number molecular weight distribution

$$M_{\mathrm{w}}=\frac{z_{\mathrm{p}}^1+\varepsilon_{\mathrm{r}}^1}{z_{\mathrm{p}}^0+\varepsilon_{\mathrm{r}}^0} \tag{44}$$

where C_{i}, C_{m}, C_{b}, C_{r}, C_{br}, T, and T_{j} are the initiator concentration, monomer concentration, butadiene concentration, radicals concentration, branched radical concentration, reactor temperature, and jacket temperature, respectively. The live polymer moments are denoted by ξ_{p}^0 and ξ_{p}^1, with first being zeroth moment, while the latter is first moment. Similarly, $\varepsilon_{\mathrm{r}}^0$ and $\varepsilon_{\mathrm{r}}^1$ are zeroth and first dead polymer moments, while $\varepsilon_{\mathrm{b}}^0$ and $\varepsilon_{\mathrm{b}}^0$ are zeroth and first butadiene moments.

The terms q_i, q_{m}, and q_{cw} represent the initiator, monomer and cooling water flow rates, respectively. V is the reactor volume, V_C is the jacket volume, while ρ is the density, C_p is the specific heat, and ΔH_{r} is the heat of reaction. Initiator efficiency is denoted by e_{f}, M_{w} is the number molecular weight, U is the global heat transfer coefficient, A is the heat transfer area, K is the Arrhenius kinetic rate constant. The superscripts d, p, i0, i1, i2, i3, fs, fb, t on the reaction rates represent the different free radical reactions steps. The superscript "in" stands for feed stream conditions, while "cw" refers to cooling water properties. The symbol "s" in the subscripts denotes styrene properties. The parameters are listed in Table 3.

Control Scheme. Two PI controllers have been implemented with the aim of controlling monomer conversion x_{m} and reactor temperature T. The manipulated variables used in order to control these variables are monomer flow rate q_{m} and cooling water flow rate q_{cw}, respectively. K_{C_1} and K_{C_2} represent the two controller gains, τ_1 and τ_2 are the time integral time constants for the two controllers, that is, tuning parameters ($\mathbf{\Lambda}=[K_{C_1}, K_{C_2}, \tau_1, \tau_2]$). The errors e_1 and e_2 for the two controllers at any time t represent the difference between the set-points (x_{m}^*, T^*) and the values at time t, that is, $x_{\mathrm{m}}(t)$, $T(t)$.

Following the descriptions provided for this process,[21] the following operational constraints have been applied to impose limits on the temperature of the reactor and the number molecular weight distribution

$$330 \le T(t) \le 420 \tag{45}$$

$$500 \le M_{\mathrm{w}}(t) \le 3000 \tag{46}$$

Process Disturbance. Following the disturbance description presented in (2), the disturbance considered for this process, $C_{\mathrm{m}}^{\mathrm{in}}$, is defined as follows

Table 3. Case Study 2: HIPS Model Parameters

Parameter	Description	Value
T^{in}	Inlet temperature	294 K
C_m^{in}	Inlet monomer concentration	8.63 mol/L
C_i^{in}	Inlet initiator concentration	0.9814 mol/L
C_b^{in}	Inlet butadiene concentration	1.0547 mol/L
V_C	Jacket volume	2000 L
ΔH_r	Heat of reaction	69919.6 J/mol
C_{ps}	Monomer heat capacity	1647.265 J/kg.K
C_{psw}	Water heat capacity	4045.7048 J/kg.K
U	Heat transfer coefiicient	80 J/(s.K.m^2)
A_{i0}	Pre-exp. factor	1.1×10^5 L^2/(mol^2.s)
A_{i1}	Pre-exp. factor	1×10^7 L/(mol.s)
A_{i2}	Pre-exp. factor	2×10^6 L/(mol.s)
A_{i3}	Pre-exp. factor	1×10^7 L/(mol.s)
A_d	Pre-exp. factor	9.1×10^{13} s^{-1}
A_{fs}	Pre-exp. factor	6.6×10^7 L/(mol.s)
A_{fb}	Pre-exp. factor	2.3×10^9 L/(mol.s)
A_t	Pre-exp. factor	1.7×10^9 L/(mol.s)
A_p	Pre-exp. factor	1×10^7 L/(mol.s)
E_{i0}	Activation energy	27340 cal/mol
E_{i1}	Activation energy	7067 cal/mol
E_{i2}	Activation energy	7067 cal/mol
E_{i3}	Activation energy	7067 cal/mol
E_d	Activation energy	29508 cal/mol
E_{fs}	Activation energy	14400 cal/mol
E_{fb}	Activation energy	18000 cal/mol
E_t	Activation energy	843 K
E_p	Activation energy	7067 cal/mol
e_f	Efficiency factor	0.57
ρ_s	Monomer density	0.915 kg/L
ρ_{cw}	Water density	1 kg/L
A	Heat transfer area	19.5 m^2
R	Ideal Gas Constant	1.9858 cal/(mol. K)

$$C_m^{in}(t) = 8.63 + 0.8\sin\left(\omega_{C_{C_m^{in},i}} t\right) \tag{47}$$

For each grade i, the critical frequency ($\omega_{C_{C_m^{in},i}}$) that produces the largest variability in x_m and T is obtained from the frequency response analysis of linearized closed-loop process model at the operating conditions specified by the optimization formulation as part of decision variables (**d**) as explained in the methodology section.

Cost Function. The capital cost of the HIPS system consists of the costs associated with the volume of the reactor and the volume of the tanks for product grades produced and can be formulated as follows

$$CC = 1200(0.1)V + \sum_{i=1}^{I} 1200(0.1)V_i \tag{48}$$

where V is the volume for the reactor, while V_i is the volume of product tank for grade i. To simplify the analysis, all the costs associated with equipment have been assigned the same value. Following (12), $W = 0.1/\text{year}$, $Z = \$1200$, $W_P = 0.1/\text{year}$, and $Z_P = \$1200$.

Moreover, the variability cost can be calculated by modifying (13) as follows

$$VC = \sum_{i=1}^{I} t_{p_i}\left(\left(\text{Max}(x_{m_i}(t)) - x_{m_i}^*\right) + \left(x_{m_i}^* - \text{Min}(x_{m_i}(t))\right)\right)35/t_{total} \tag{49}$$

where, $x_{m_i}^*$ is the product grade specification, $x_{m_i}(t)$ is the value at time t for the monomer conversion, while the penalty for variability has been assigned the value of \$35 per unit deviation in conversion set point per unit time. The operating cost for this process can be calculated as follows

$$OC = \sum_{i=1}^{I} t_{p_i}\left(20(\overline{q_{cw_i}}) + 30(\overline{q_{m_i}})\right)/t_{total} \tag{50}$$

where $\overline{q_{cw}}$ and $\overline{q_m}$ are the steady-state values for cold water flow and monomer flow at production of each grade i, which are weighted by the respective costs per unit, that is, \$20/(L) min and \$30/(L) min.

Furthermore, the transition cost can be calculated from (15) as follows, that is

$$TC = \sum_{i=1}^{I} 35 t_i \text{SSE}_i / t_{total} \tag{51}$$

where SSE_i is the sum of squared errors during transition period of the grade i. The penalty for waste production has been assigned the value of \$35 per unit squared error in conversion per unit time. The decision variables related to the design, control, and scheduling aspects are evaluated for the optimal solution. The volume of the reactor and inlet temperature T^{in} ($\boldsymbol{\kappa} = [V, T^{in}]$) are the design decision variable, while tuning parameters for the two PI controllers ($\boldsymbol{\Lambda} = [K_{C_1}, K_{C_2}, \tau_1, \tau_2]$) are the control decision variables to be evaluated. The scheduling decision variables include slopes for transition of each grade, that is, $\alpha_1, \alpha_2, \alpha_3, \alpha_4$ and optimal sequence of production, that is, **s**.

Following the developments described above, the optimization formulation shown in (16) is solved with the specifications of HIPS system described above. The specifications of four different grades are shown in Table 4 along with the information related to the critical scenarios created for uncertainty in the product demands. The results obtained for the integration of scheduling, design, and control of the HIPS case study are shown in Table 5. Figure 7a depicts the transition and production of various grades under the critical realizations in the disturbance (C_m^{in}) for the production demand uncertainty scenario that presented the maximum variability in the monomer conversion. To validate the linear approximation used to generate worst-case variability, a test has been performed where process constraints have been evaluated for the range of frequencies. The range includes minimum, maximum, and the critical frequency obtained from the linear approximation proposed in this work. For this range of frequencies, the profiles of number average molecular weight for the uncertain demand scenario that correspond to the maximum variability in the controlled variable are shown in Figure 7b. It is clear from the figure that the largest variability in this variable corresponds to the critical frequency and constraints are not violated over a range of frequencies. Thus, the linear approximation used in this work to identify the worst-case variability in the controlled variables is a practical and suitable approach to address the optimal design of large-scale highly nonlinear systems such as that presented in this case study.

The CPU time required for the second case study was very high as compared to case study 1 because of the presence of nonlinearity and the size of the problem. Each single function evaluation takes around 205 s, while it took approximately 8 h to generate the solution for this case study. The approach presented here assumes a fixed flow sheet of the process as well as a fixed control scheme whereas the scheduling decisions (sequence of product grades) were made for 3–4 grades in the case studies. Moreover, the multiscenario

Table 4. Case Study 2: Product Specifications and Demand Scenarios, HIPS

Grade	Monomer Conversion
1	0.25
2	0.30
3	0.35
4	0.40

Scenario	Demands of Product Grades: 1, 2, 3,4 (L)	Probability
1	10,000, 10,000, 10,000, 10,000	0.4
2	15,000, 12,000, 7000, 5000	0.3
3	7000, 15,000, 5000, 12,000	0.2
4	5000, 12,000, 15,000, 7000	0.1

approach was used to handle uncertainty only in product demands in the two case studies. All these factors keep the computational efforts within reasonable limits. The application of multiscenario approach to handle uncertainty increases the computational time as more uncertain parameters are added into the analysis. Similarly, adding more integer decision variables to account for structural decisions related to process flow sheet and control structure selection will further increase the methodology's computational time.

The results from the case study demonstrate the capability of the methodology to be applied to a large scale nonlinear problem in the presence of process disturbances with oscillatory behavior at critical frequency determined for production each grade, while uncertainty has been addressed in product demands.

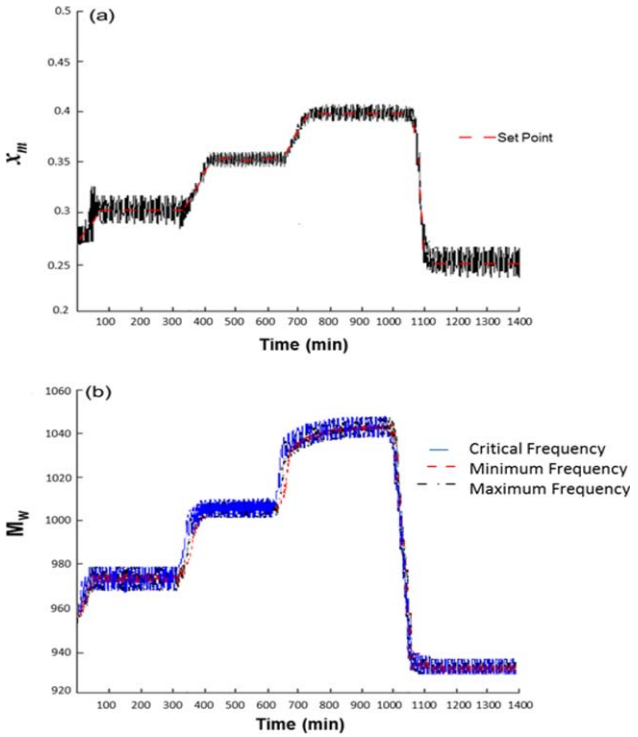

Figure 7. HIPS case study: (a) transition and production of grade for the scenario with maximum variability; (b) process constraints evaluated for the range of frequencies.

[Color figure can be viewed in the online issue, which is available at wileyonlinelibrary.com.]

Conclusions

A methodology for integration of design, scheduling, and control for the multiproduct processes has been presented. The key novelty introduced by the present methodology is that it explicitly addresses the scheduling, design, and control simultaneously while taking into account the influence of process disturbances and uncertainty in the parameters, which aims to represent the actual operation of these processes. The process disturbances are specified as sinusoidal signals at critical frequency, which are determined via frequency response analysis. The uncertainty in the parameter has been addressed via multiscenario approach, where critical scenarios were created and probability of occurrence was assigned for each of them. Another feature of study is in terms of smooth transitions between different product grades. Ramp functions have been used for the transition and the slopes of these ramps which determine the rate of transitions were part of decision variables.

Two case studies were developed with first case study focusing in the comparison of a semisequential approach to the simultaneous methodology developed in this work for the integration of scheduling, design, and control. The second case study tests the capability of the methodology in the application of larger nonlinear process. The results from this case study show that the methodology developed in this work is a practical approach that can integrate the scheduling, design, and control aspects of the large multiproduct processes.

Table 5. Case Study 2: HIPS Results

Decision Variables and Costs	Optimal Values
Design:	
V (L)	7174
T^{in} (K)	387.74
Control:	
$K_{C_1}, K_{C_2}, \tau_1, \tau_2$	−1.732, −0.0183, 1132, 23
Scheduling:	
s (sequence of grades)	2–3-4-1
$\alpha_1, \alpha_2, \alpha_3, \alpha_4$ (transition slopes)	0.0124, 0.0386, 0.0213, −0.0311
Capital Cost (M$/year)	5.256
Operating Cost (M$/year)	1.766
Variability Cost (M$/year)	0.193
Transition Cost (M$/year)	0.870
Total Cost (M$/year)	7.128

Acknowledgment

The authors would like to acknowledge the financial support provided by the Natural Sciences and Engineering Research Council of Canada (NSERC).

Notation

f = open-loop dynamic process model
g = controller equations
$\mathbf{f}_{closed}$ = closed-loop process model (open-loop process model **f** and control scheme **g**)
$\boldsymbol{\varphi}$ = process inputs
u = manipulated variables used by the controller
w = uncertain parameters
$\boldsymbol{\eta}$ = process disturbance
$\boldsymbol{\Omega}$ = process output variables
y = process output variables that are in closed-loop (controlled variables)
$\boldsymbol{\theta}$ = process output variables that are not in closed-loop
d = optimization variables

$\boldsymbol{\kappa}$ = design parameters and operating conditions
$\boldsymbol{\Lambda}$ = controller tuning parameters
$\boldsymbol{\alpha}$ = transition slopes
$\mathbf{s}$ = production sequence
$\mathbf{S}$ = scheduling parameters ($\mathbf{s}$ and $\boldsymbol{\alpha}$)
$\varnothing$ = cost function
$\mathbf{h}$ = process constraints
i = index denoting product grade
k = index denoting process disturbance
z = index denoting uncertainty scenarios
l = index denoting controlled variable
P^z = probability associated with uncertainty scenario z
$\omega_{c_{k,i}}$ = critical frequency of disturbance k affecting grades i
I = number of grades of products to be produced
$\mathbf{x}(\mathbf{t})$ = system's states
$\mathbf{c}(\mathbf{t})$ = controllers' states
AR = amplitude ratio
C_i^{SP} = product specification for grade i

Literature Cited

1. Kiraly LM, Friedler F, Szoboszlai L. Optimal design of multipurpose batch chemical plants. *Comput Chem Eng*. 1989;13(4–5):527–534.
2. Wang CF, Quan HY, Xu X. Optimal design of multiproduct batch chemical processes using tabu search. *Comput Chem Eng*. 1999;23(3):427–437.
3. Wang CF, Quan HY, Xu X. Optimal design of multiproduct batch chemical process using genetic algorithms. *Ind Eng Chem Res*. 1996;35(10):3560–3566.
4. Cantrell JG, Luyben, WL. Design of rapid-transition multiproduct processes. *Ind Eng Chem Res*. 1996;35(8):2624–2631.
5. White V, Perkins JD, Espie DM. Switchability analysis. *Comput Chem Eng*. 1996;20(4):469–474.
6. Kamesh R, Reddy PS, Rani KY. Comparative study of different cascade control configurations for a multiproduct semibatch polymerization reactor. *Ind Eng Chem Res*. 2014;53(38):14735–14754.
7. Yi G, Reklaitis GV. Adaptive model predictive inventory controller for multiproduct warehouse system. *Automatica*. 2014;50(9):2245–2253.
8. Rani KY. Sensitivity compensating nonlinear control: exact model based approach. *J Process Control*. 2012;22(3):564–582.
9. Zeballos LJ, Novas JM, Henning GP. A CP formulation for scheduling multiproduct multistage batch plants. *Comput Chem Eng*. 2011;35(12):2973–2989.
10. Liberopoulos G, Kozanidis G, Hatzikonstantinou O. Production scheduling of a multi-grade PET resin plant. *Comput Chem Eng*. 2010;34(3):387–400.
11. Shi B, Yan LX, Wu W. Rule-based scheduling of single-stage multiproduct batch plants with parallel units. *Ind Eng Chem Res*. 2012;51(25):8535–8549.
12. Fumero Y, Corsano G, Montagna JM. Scheduling of multistage multiproduct batch plants operating in a campaign-mode. *Ind Eng Chem Res*. 2012;51(10):3988–4001.
13. Liu SS, Pinto JM, Papageorgiou LG. Single-stage scheduling of multiproduct batch plants: an edible-oil deodorizer case study. *Ind Eng Chem Res*. 2010;49(18):8657–8669.
14. Alarcia F, De la Cal JC, Asua JM. Scheduling the production of a portfolio of emulsion polymers in a single CSTR. *Ind Eng Chem Res*. 2006;45(10):3711–3717.
15. Janak SL, Lin XX, Floudas CA. A new robust optimization approach for scheduling under uncertainty - II. Uncertainty with known probability distribution. *Comput Chem Eng*. 2007;31(3):171–195.
16. Li J, Floudas CA. Optimal event point determination for short-term scheduling of multipurpose batch plants via unit-specific event-based continuous-time approaches. *Ind Eng Chem Res*. 2010;49(16):7446–7469.
17. Shaik MA, Janak SL, Floudas CA. Continuous-time models for short-term scheduling of multipurpose batch plants: a comparative study. *Ind Eng Chem Res*. 2006;45(18):6190–6209.
18. Alvarado-Morales M, Abd Hamid MK, Sin G, Gernaey KV, Woodley JM, Gani R. A model-based methodology for simultaneous design and control of a bioethanol production process. *Comput Chem Eng*. 2010;34(12):2043–2061.
19. Ramos Manuel A, Gomez Jorge M, Jean-Michel R. Simultaneous optimal design and control of an extractive distillation system for the production of fuel grade ethanol using a mathematical program with complementarity constraints. *Ind Eng Chem Res*. 2014;53(2):752–764.
20. Ricardez-Sandoval LA, Budman HM, Douglas PL. Simultaneous design and control of chemical processes with application to the Tennessee Eastman process. *J Process Control*. 2009;19(8):1377–1391.
21. Lamanna R, Vega P, Revollar S, Alvarez H. Simultaneous design and control of a sugar cane sulfitation tower. *Rev Iberoam Autom E Inform Ind*. 2009;6(3):32.
22. Sanchez-Sanchez K, Ricardez-Sandoval L. Simultaneous process synthesis and control design under uncertainty: a worst-case performance approach. *AIChE J*. 2013;59(7):2497–2514.
23. Flores-Tlacuahuac A, Biegler LT. Integrated control and process design during optimal polymer grade transition operations. *Comput Chem Eng*. 2008;32(11):2823–2837.
24. Asteasuain M, Bandoni A, Sarmoria C, Brandolin A. Simultaneous process and control system design for grade transition in styrene polymerization. *Chem Eng Sci*. 2006;61(10):3362–3378.
25. Asteasuain M, Bandoni A, Sarmoria C, Brandolin A. Simultaneous design and control of a semibatch styrene polymerization reactor. *Ind Eng Chem Res*. 2004;43(17):5233–5247.
26. Lopez-Negrete de la Fuente R, Flores-Tlacuahuac A. Integrated design and control using a simultaneous mixed-integer dynamic optimization approach. *Ind Eng Chem Res*. 2009;48(4):1933–1943.
27. Ricardez-Sandoval LA, Budman HM, Douglas PL. Application of robust control tools to the simultaneous design and control of dynamic systems. *Ind Eng Chem Res*. 2009;48(2):801–813.
28. Flores-Tlacuahuac A, Biegler LT. Simultaneous mixed-integer dynamic optimization for integrated design and control. *Comput Chem Eng*. 2007;31(5–6):588–600.
29. Sharifzadeh M, Thornhill NF. Integrated design and control using a dynamic ac inversely controlled process model. *Comput Chem Eng*. 2013;48(10):121–134.
30. Mohideen MJ, Perkins JD, Pistikopoulos EN. Optimal design of dynamic systems under uncertainty. *AIChE J*. 1996;42(8):2251–2272.
31. Kookos IK, Perkins JD. An algorithm for simultaneous process design and control. *Ind Eng Chem Res*. 2001;40(19):4079–4088.
32. Bahakim SS, Ricardez-Sandoval LA. Simultaneous design and MPC-based control for dynamic systems under uncertainty: a stochastic approach. *Comput Chem Eng*. 2014;63(17):66–81.
33. Gutierrez G, Ricardez-Sandoval LA, Budman HM, Prada C. An MPC-based control structure selection approach for simultaneous process and control design. *Comput Chem Eng*. 2014;70(SI):11–21.
34. Sanchez-Sanchez KB, Ricardez-Sandoval LA. Simultaneous design and control under uncertainty using model predictive control. *Ind Eng Chem Res*. 2013;52(13):4815–4833.
35. Chawankul N, Ricardez-Sandoval LA, Budman HM, Douglas RL. Integration of design and control: a robust control approach using MPC. *Can J Chem Eng*. 2007;85(4):433–446.
36. Francisco M, Vega P, Alvarez H. Robust integrated design of processes with terminal penalty model predictive controllers. *Chem Eng Res Des*. 2011;89(7):1011–1024.
37. Vega P, Lamanna R, Revollar S, Francisco M. Integrated design and control of chemical processes – part II: an illustrative example. *Comput Chem Eng*. 2014;71:618–635.
38. Ricardez-Sandoval LA. Optimal design and control of dynamic systems under uncertainty: a probabilistic approach. *Comput Chem Eng*. 2012;43:91–107.
39. Ricardez-Sandoval LA, Douglas PL, Budman HM. A methodology for the simultaneous design and control of large-scale systems under process parameter uncertainty. *Comput Chem Eng*. 2011;35(2):307–318.
40. Ricardez Sandoval LA, Budman HM, Douglas PL. Simultaneous design and control of processes under uncertainty: a robust modelling approach. *J Process Control*. 2008;18(7–8):735–752.
41. Sakizlis V, Perkins JD, Pistikopoulos EN. Parametric controllers in simultaneous process and control design optimization. *Ind Eng Chem Res*. 2003;42(20):4545–4563.
42. Mohideen MJ, Perkins JD, Pistikopoulos EN. Optimal synthesis and design of dynamic systems under uncertainty. *Comput Chem Eng*. 1996;20:S895–S900.
43. Bansal V, Perkins JD, Pistikopoulos EN, Ross R, van Schijndel JMG. Simultaneous design and control optimisation under uncertainty. *Comput Chem Eng*. 2000;24(2–7):261–266.
44. Yuan ZH, Chen BZ, Sin G, Gani R. State-of-the-art and progress in the optimization-based simultaneous design and control for chemical processes. *AIChE J*. 2012;58(6):1640–1659.

45. Sharifzadeh M. Integration of process design and control: a review. *Chem Eng Res Des*. 2013;91(12):2515–2549.
46. Sakizlis V, Perkins JD, Pistikopoulos EN. Recent advances in optimization-based simultaneous process and control design. *Comput Chem Eng*. 2004;28(10):2069–2086.
47. Ricardez-Sandoval LA, Budman HM, Douglas PL. Integration of design and control for chemical processes: a review of the literature and some recent results. *Annu Rev Control*. 2009;33(2):158–171.
48. Vega P, Lamanna R, Revollar S, Francisco M. Integrated design and control of chemical processes – part II: an illustrative example. *Comput Chem Eng*. 2014;71:602–617.
49. Fumero Y, Montagna JM, Corsano G. Simultaneous design and scheduling of a semicontinuous/batch plant for ethanol and derivatives production. *Comput Chem Eng*. 2012;36:342–357.
50. Jayaraman VK, Kulkarni BD, Karale S, Shelokar P. Ant colony framework for optimal design and scheduling of batch plants. *Comput Chem Eng*. 2000;24(8):1901–1912.
51. Castro PM, Barbosa-Povoa AP, Novais AQ. Simultaneous design and scheduling of multipurpose plants using resource task network based continuous-time formulations. *Ind Eng Chem Res*. 2005;44(2):343–357.
52. Voudouris VT, Grossmann IE. MILP model for scheduling and design of a special class of multipurpose batch plants. *Comput Chem Eng*. 1996;20(11):1335–1360.
53. Lin X, Floudas CA. Design, synthesis and scheduling of multipurpose batch plants via an effective continuous-time formulation. *Comput Chem Eng*. 2001;25(4–6):665–674.
54. Heo SK, Lee KH, Lee HK, Lee IB, Park JH. A new algorithm for cyclic scheduling and design of multipurpose batch plants. *Ind Eng Chem Res*. 2003;42(4):836–846.
55. Birewar DB, Grossmann IE. Incorporating scheduling in the optimal design of multiproduct batch plants. *Comput Chem Eng*. 1989;13(1–2):141–161.
56. Pinto-Varela T, Barbosa-Povoa A, Ana Paula FD, Novais AQ. Design and scheduling of periodic multipurpose batch plants under uncertainty. *Ind Eng Chem Res*. 2009;48(21):9655–9670.
57. Bhatia TK, Biegler LT. Dynamic optimization for batch design and scheduling with process model uncertainty. *Ind Eng Chem Res*. 1997;36(9):3708–3717.
58. Zhuge J, Ierapetritou MG. Integration of scheduling and control for batch processes using multi-parametric model predictive control. *AIChE J*. 2014;60(9):3169–3183.
59. Chu Y, You F. Moving horizon approach of integrating scheduling and control for sequential batch processes. *AIChE J*. 2014;60(5):1654–1671.
60. Terrazas-Moreno S, Flores-Tlacuahuac A, Grossmann IE. Lagrangean heuristic for the scheduling and control of polymerization reactors. *AIChE J*. 2008;54(5):163–182.
61. Terrazas-Moreno S, Flores-Tlacuahuac A, Grossmann IE. Simultaneous cyclic scheduling and optimal control of polymerization reactors. *AIChE J*. 2007;53(9):2301–2315.
62. Angel Gutierrez-Limon M, Flores-Tlacuahuac A, Grossmann IE. A multiobjective optimization approach for the simultaneous single line scheduling and control of CSTRs. *Ind Eng Chem Res*. 2012;51(17):5881–5890.
63. Flores-Tlacuahuac A, Grossmann IE. Simultaneous cyclic scheduling and control of a multiproduct CSTR. *Ind Eng Chem Res*. 2006;45(20):6698–6712.
64. de Prada C, Rodriguez M, Sarabia D. On-line scheduling and control of a mixed continuous-batch plant. *Ind Eng Chem Res*. 2011;50(9):5041–5049.
65. Flores-Tlacuahuac A, Grossmann IE. Simultaneous cyclic scheduling and control of tubular reactors: single production lines. *Ind Eng Chem Res*. 2010;49(22):11453–11463.
66. Flores-Tlacuahuac A, Grossmann IE. Simultaneous scheduling and control of multiproduct continuous parallel lines. *Ind Eng Chem Res*. 2010;49(17):7909–7792.
67. Engell S, Harjunkoski I. Optimal operation: scheduling, advanced control and their integration. *Comput Chem Eng*. 2012;47:121–133.
68. Harjunkoski I, Nystroem R, Horch A. Integration of scheduling and control-theory or practice? *Comput Chem Eng*. 2009;33(12):1909–1918.
69. Terrazas-Moreno S, Flores-Tlacuahuac A, Grossmann IE. Simultaneous design, scheduling, and optimal control of a methyl-methacrylate continuous polymerization reactor. *AIChE J*. 2008;54(12):3160–3170.
70. Jiao Y, Su H, Hou W, Liao Z. A multiperiod optimization model for hydrogen system scheduling in refinery. *Ind Eng Chem Res*. 2012;51(17):6085–6098.
71. Menezes BC, Kelly JD, Grossmann IE. Improved swing-cut modeling for planning and scheduling of oil-refinery distillation units. *Ind Eng Chem Res*. 2013;52(51):18324–18333.
72. Patil BP, Fukasawa R, Ricardez-Sandoval LA. Scheduling of operations in a large-scale scientific services facility via multicommodity flow and an optimization-based algorithm. *Ind Eng Chem Res*. 2015;54(5):1628–1639.

Manuscript received Jan. 2, 2015, and revision received Feb. 24, 2015.